Near-ultraviolet emission bands of Li—rare-gas molecules

W. J. Wang and M. D. Havey
Physics Department, Old Dominion University, Norfolk, Virginia 23508
(Received 28 October 1983)

Near-ultraviolet emission bands have been observed in Li-Ar, Li-Kr, and Li-Xe mixtures. The bands are due to transitions from bound molecular Li—rare-gas states associated with the atomic Li $3d$, $3p$, and $3s$ states and ground-state rare-gas atoms. The transitions are all to the dissociative Li—rare-gas $2s\sigma$ molecular ground state. The Li-Ar, Li-Kr, and Li-Xe $3s\sigma$-$2s\sigma$ collision-induced bands are progressively shifted, for the heavier rare gases, further to the red of the asymptotic atomic Li $3s$-$2s$ energy difference. For Li-Xe this shift is a remarkable 4000 cm^{-1}. We also report rate coefficients for quenching, by all the rare gases, of the atomic Li $3d$ and $3p$ states.

I. INTRODUCTION

The discovery several years ago of intense collision-induced emission bands in alkali-atom—rare-gas mixtures[1,2] has stimulated a number of studies of excited molecular states in these systems.[3–7] The interest stems partly from the realization that the excited states can exhibit substantial binding and should lend themselves to analysis using semiclassical, line-broadening models or be amenable to conventional spectroscopic investigations. A principal goal of the studies is to obtain potential energy curves and dipole moments for the states responsible for the observed emission bands.[8–11] These quantities are useful in descriptions of a wide range of physical phenomena, including line broadening, quenching, and depolarization processes.

There is also some possibility for observing laser action[12] in the collision-induced bands. The bands correspond to excimer transitions in the alkali-atom—rare-gas molecular systems and may have oscillator strengths as large as 10^{-1} at some internuclear separations.[8] Furthermore, it appears that for some systems, at high rare-gas pressures, most excitation above the alkali-atom resonance state is channeled into these intense bands.

Such collision-induced features have been observed in emission, and in some cases in absorption, for all the A-R systems[13] (A = alkali atom; R = Ar, Kr, Xe) except Li-R. We report in this paper the results of our observations of collision-induced emission bands in Li-R mixtures. We have measured the shapes and positions of these spectral features for Li-Ar, Li-Kr, and Li-Xe. Also among our observations are measurements of the rare-gas pressure dependence of the population in the atomic Li states giving rise to the bands. In particular, we have measured the rate coefficient for collisional mixing, by all the rare gases, of the atomic Li $3d$ and $3p$ states. We have also measured the rate coefficient for quenching of the Li $3p$ state to states other than the $3d$ state. The pressure dependence of the collision-induced bands relative to selected atomic Li emission lines has also been determined.

II. EXPERIMENT

Our experimental scheme is most easily understood with reference to Fig. 1. In this scheme atomic Li is produced in the $3d$ state by stepwise excitation via the $2p$ resonance state. Collisions between Li ($3d$) and rare-gas atoms then relax the excited Li to the $3p$ and $3s$ states. The $3s$ state is also populated by radiative transitions from the collisionally populated $3p$ state. Subsequent three-body collisions with rare-gas atoms produce bound Li-R molecules in the various molecular states associated with the atomic Li excited states shown in Fig. 1 and ground-state rare-gas atoms. The relative intensities of the $3d$-$2p$, $3p$-$2s$, and $3s$-$2p$ transitions serve to monitor the population in the various $n=3$ atomic Li states. The emission intensity in the collision-induced bands measures the relative population produced in the relevant molecular Li-R states. In the remainder of this paper, we will ignore the effect of the molecular on the atomic populations. This approximation is justified by the fact that for our experiments only a few percent, at most, of the total excited population is in molecular form.[14] Of course, the effect of the atomic on the molecular populations cannot be ignored; the excited atomic Li is the source of the bound molecular Li—rare-gas molecules that are eventually

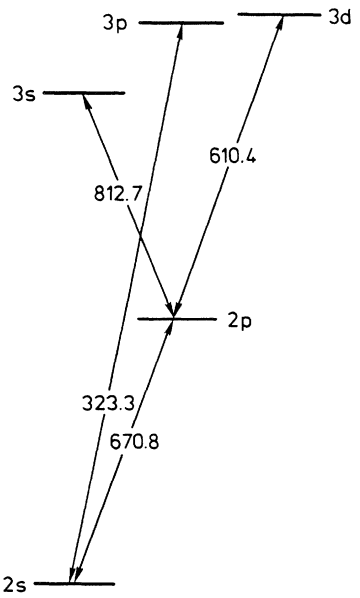

FIG. 1. Energy-level diagram for the lowest few states in Li.

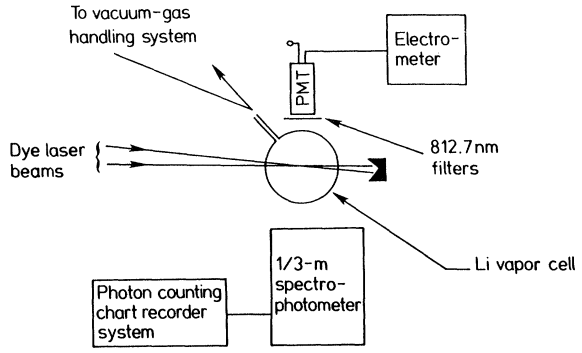

FIG. 2. Schematic diagram of the experimental apparatus.

created by three-body Li-R collisions. The degree of relaxation and the intensity of the collision-induced bands depend strongly on the rare gas. The details of each case will be discussed in a later section of this paper.

The experimental arrangement used to observe the atomic and molecular emission is shown in Fig. 2. Atomic Li is excited to the $3d$ state by two broad band, cw dye lasers. Each laser has an output power of about 500 mw in a band width less than 0.5 cm^{-1}. The laser beams overlap in an approximately 1-cm^3 volume near the center of the Li vapor cell. The cell and its operation have been described previously;[15] it produces a usable Li density in the $10^{-7}-10^{-4}$ Torr range at a cell temperature of about 40°C. The cell is connected to a vacuum-gas handling system which facilitates rapid gas and pressure changes and which monitors the cell pressure. The background pressure in the cell is about 10^{-6} Torr.

The red emission from the vapor is detected by a filtered PMT (photomultiplier tube) which measures the relative $3s$-$2p$ atomic Li emission at 812.7 nm. The output from the PMT is monitored by an electrometer. The bluer emission ($\lambda < 650$ nm), which consists of atomic emission on the $3d$-$2p$ (610.4 nm) and $3p$-$2s$ (323.2 nm) transitions and the molecular-emission bands, is spectrally dispersed by a $\frac{1}{3}$-m monochromator with a resolution of approximately 10 Å. The monochromator throughput is detected and recorded on a PMT-chart recorder system. This PMT has an S-20 cathode and is operated in the photon-counting mode.

III. RESULTS AND DISCUSSION

In general, when we excited the Li $3d$ state, we observed atomic emission on the $3d$-$2p$, $3p$-$2s$, and $3s$-$2p$ Li transitions (see Fig. 1.) We observed no emission from states above the $3d$. In addition, we discovered in Li-Ar, Li-Kr, and Li-Xe mixtures intense emission bands in the spectral range 360—440 nm. We attribute this continuum emission to collision-induced bands of the associated Li—rare-gas molecules. All observed features required that both lasers be tuned to resonance and each appeared sharply upon laser tuning into resonance. Emission intensities were linear in laser power and were substantially different for the different rare gases. Ratios of atomic emission line intensities were independent of Li density, indicating an absence of radiation trapping in our experiments.

The specific results of our studies divide naturally into two parts. In the first, we present our data on collisional relaxation, by the rare gases, of the excited Li $3d$ state population. In the second, we describe the results of our observations on the collision-induced Li-R emission bands.

A. Collisional quenching in the Li $3d,3p$ states

As mentioned previously, the relaxation of the excited Li atomic populations can be discussed independent of the bound molecular populations. At the rare-gas pressures used in our experiments (< 100 Torr), only a few percent of the excited population will reside in bound molecular states.[14] A simple rate equations analysis shows that, under these circumstances, the ratio of the intensities of the $3p$-$2s$ and $3d$-$2p$ atomic transitions is given by

$$\frac{I(3d\text{-}2p)}{I(3p\text{-}2s)} = G\left[\frac{\Gamma_{3p\text{-}3d}+\Gamma_{3p\text{-}3s}}{\Gamma_{3d\text{-}3p}} + \frac{\gamma_{3p\text{-}3s}+\gamma_{3p\text{-}2s}}{\Gamma_{3d\text{-}3p}}\right]. \quad (1)$$

In this expression we have taken any quenching of the $3p$ state to be to the relatively nearby $3s$ state. This is consistent with expectations based on existing Li-R potentials[9] for these states. The quantity G is a geometrical factor, the quantities Γ are mixing rates between the indicated states, and γ represents radiative decay rates. Note that $\Gamma_{3d\text{-}3p}/\Gamma_{3p\text{-}3d} = \frac{3}{5}\exp(\Delta/kT)$, where Δ is the $3d$-$3p$ energy separation (357.7 cm^{-1}). As Γ is proportional to pressure P according to $\Gamma = kP$ (k is a rate coefficient), a plot of this intensity ratio against $1/P$ yields a straight line of slope $G/k_{3d\text{-}3p}$ and intercept $G(k_{3p\text{-}3d}+k_{3p\text{-}3s})/k_{3d\text{-}3p}$.

It has been possible in our experiments to determine the factor G, allowing us to extract both $k_{3p\text{-}3d}$ and $k_{3p\text{-}3s}$ from our data. As will be discussed, the quenching rate $\Gamma_{3p\text{-}3s}$ is very small for Li-He collisions. This means that the intercept in a plot of (1) for He, as shown in Fig. 3, is given by $Gk_{3p\text{-}3d}/k_{3d\text{-}3p}$. The ratio of rate coefficients is known from detailed balancing, so G can be determined from this data. We obtain a value of 5.6(6) for G. Now, G is a quantity depending on the arrangement of our

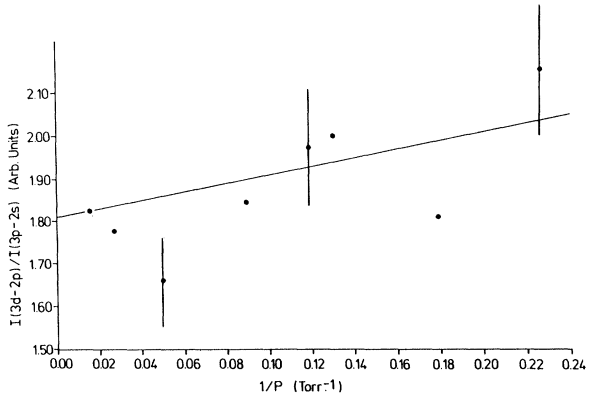

FIG. 3. Relative intensities of the Li $3d$-$2p$ and $3p$-$2s$ transitions vs (pressure)$^{-1}$ for He buffer gas.

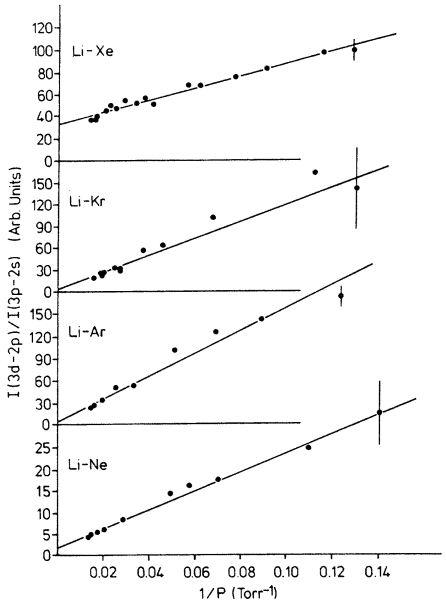

FIG. 4. Relative intensities of the Li $3d$-$2p$ and $3p$-$2s$ transition vs (pressure)$^{-1}$ for Ne, Ar, Kr, and Xe buffer gases. The relative intensity scale has been normalized as described in the text. Note the different intensity scales for each gas.

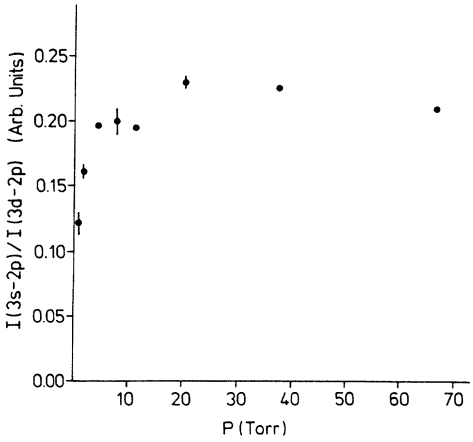

FIG. 5. Relative intensities of the atomic Li $3s$-$2p$ and $3d$-$2p$ transitions vs He gas pressure.

detectors and the usual intensity factors; it does not depend on the rare gas. We thus use G as determined in Li-He experiments to put the ratio (1) on an absolute scale for all the rare gases. Plots of our data, as in (1), for Li-Ne, Li-Ar, Li-Kr, and Li-Xe are presented in Fig. 4. Linear least-squares fits of $I(3d\text{-}2p)/I(3p\text{-}2s)$ versus $1/P$ allowed us to determine the rate coefficients $k_{3d\text{-}3p}$ and $k_{3p\text{-}3s}$. Tabulated values of the relevant radiative rates[16] were used in these fits. Values of the rate coefficients thus obtained are presented in Table I.

To confirm the absence of quenching of the $3p$ state for He, we have measured the ratio $I(3s\text{-}2p)/I(3d\text{-}2p)$ as a function of pressure; our data are presented in Fig. 5. A steady-state rate equations analysis yields

$$I(3s\text{-}2p)/I(3d\text{-}2p)=G'\frac{(\gamma_{3p\text{-}3s}+\Gamma_{3p\text{-}3s})(\Gamma_{3d\text{-}3p})}{\gamma_R+\Gamma_{3p\text{-}3d}+\Gamma_{3p\text{-}3s}}\ , \qquad (2)$$

where G' is a constant and γ_R the total radiative decay rate of the $3p$ state. The data of Fig. 5 can only be adequately described by (2) if $\Gamma_{3p\text{-}3s} \ll \gamma_{3p\text{-}3s}$; the ratio would increase as P at high pressure if this was not true. Including quenching of the $3s$ or $3d$ state does not alter this conclusion, and we are justified in neglecting $\Gamma_{3p\text{-}3s}$ in (1) when determining G.

Table I summarizes our results for the rate coefficients $k_{3d\text{-}3p}$ and $k_{3p\text{-}3s}$ and for average cross sections $\bar{\sigma}=k/\bar{v}$, where $\bar{v}$ is the average thermal velocity at our experimental temperature of 40 °C. Also included are available values of the cross sections obtained by other workers.[17,18] Our results can qualitatively be discussed on the basis of relevant interatomic potentials calculated by Pascale and Vandeplanque.[9] The near proximity of the $3s\sigma$ and $3p\pi$ potentials at small internuclear separations can lead to the $3p \rightarrow 3s$ quenching that we observe. The mixing of the molecular states could be due either to Coriolis (rotational) interactions or to dynamical mixing associated with a curve crossing in this range of internuclear separations. The calculated potentials show a rapid separation of the $3s\sigma$ and $3p\pi$ potentials as one goes to lighter rare gases; the cross sections also decrease rapidly as one would expect.

The $3d$-$3p$ quenching can generally be understood in terms of similar mechanisms. There is a crossing of the $3p\sigma$ and $3d\delta$ states in the region of the attractive well for all the Li-R potentials except Li-He; rotational mixing should be important for all cases. The dependence of the cross sections on the rare gas is not, on the basis of existing potentials, obvious. It has been suggested[19] that the

TABLE I. Rate coefficients and cross sections for rare-gas $3d$-$3p$ and $3p$-$3s$ quenching in atomic Li.

	Our results				Other results
	$K(3d\text{-}3p)$	$K(3p\text{-}3s)$	$\sigma(3d\text{-}3p)$	$\sigma(3p\text{-}3s)$	$\sigma(3d\text{-}3p)$
Species	(cm^3/s)	(cm^3/s)	(Å^2)	(Å^2)	(Å^2)
Li-He	$8.3(4.4)\times10^{-10}$		52(28)		9.0
Li-Ne	$3.8(5)\times10^{-12}$		$3.4(4)\times10^{-1}$		1.2
Li-Ar	$5.0(7)\times10^{-13}$	$1.6(1.2)\times10^{-13}$	$4.8(6)\times10^{-2}$	$1.5(1.2)\times10^{-2}$	$>4\times10^{-3}$
Li-Kr	$6.9(9)\times10^{-13}$	$3.0(1.1)\times10^{-13}$	$6.8(9)\times10^{-2}$	$3.0(1.1)\times10^{-2}$	
Li-Xe	$1.4(2)\times10^{-12}$	$8.0(1.4)\times10^{-12}$	$1.4(2)\times10^{-1}$	$8.0(1.0)\times10^{-1}$	

large difference between the He and Ne cross sections can be explained on the basis of a model viewing the collision as one between the rare gas and the Li valence electron. Although this seems to be a reasonable possibility, systematic calculations seem to offer the best hope for understanding the variation of σ with rare gas.

The measurements of other workers,[17,18] which are also summarized in Table I, were done at a temperature of 650 °C, and so direct comparisons are not really meaningful. It does appear that the Li-He and Li-Ne $3d$-$3p$ quenching is not strongly temperature dependent; however, if the velocity dependence of the rate coefficients is structured, even this may not be true.

B. Collision-induced emission bands

The molecular emission spectra observed in Li-Ar, Li-Kr, and Li-Xe mixtures are presented in Fig. 7. The position of the maximum emission intensity and the full width at half maximum for each band is given in Table II. The origin of these spectral features can be understood with reference to Fig. 6. As has been discussed, excitation of the Li $3d$ state produces atomic population in the Li $3d$, $3p$, and $3s$ states. It is well known[15] that three-body collisions between two rare-gas atoms and an excited Li atom can produce bound Li–rare-gas molecules in the molecular states correlating to each of the atomic states above. The bound population then can decay radiatively (or otherwise) via a number of transitions, including excimer transitions to the repulsive $2s\sigma$ molecular ground state.

We believe that the observed bands are indeed excimer emission from excited states of Li-R molecules, and a number of points and observations support this view. First, the positions of the emission peaks depend strongly on the rare gas and are, on the basis of existing potentials,[9] in approximately the positions one would expect. These positions are summarized in Table II. Second, the peak intensity of each band, relative to the atomic Li $3p$-$2s$ emission line intensity, is independent of Li density. This eliminates Li_2 as a possible source of the spectra, for the relative intensity of the band to atomic emission would grow as [Li] in that case.

Finally, the redmost band grows as the square of the R pressure relative to the $3s$-$2p$ atomic Li emission; this is consistent with the three-body formation of molecular Li-R in the $3s\sigma$ state which correlates to the atomic Li $3s$ state. This behavior is illustrated, for the single observed Li-Xe band, in Fig. 8. The redder of the two observed bands for Li-Ar and Li-Kr also grows linearly at the expense of the bluer, indicating molecular states above the $3s\sigma$ are responsible for the emission. As only the $3d$ and $3p$ Li states are populated, one or several of the molecular states associated with these must give rise to the observed emission. From our measurements, we cannot distinguish among these possibilities.

We have also observed that the wavelength of peak intensity and the full width at half maximum of each ob-

TABLE II. Peaks and widths of continuum emission bands observed in Li-R mixtures. The predicted peak positions are the wavelengths of emission from the minimum of the $3s\sigma$ potential to the repulsive $2s\sigma$ potential; the potentials are from Ref. 9.

Species	Emission peak position	Width	Predicted peak position
Li-Ar	380(2)	20(1)	
	411(2)	14(1)	396
Li-Kr	392(2)	19(2)	
	416(2)	13(1)	405
Li-Xe	431(2)	12(1)	414

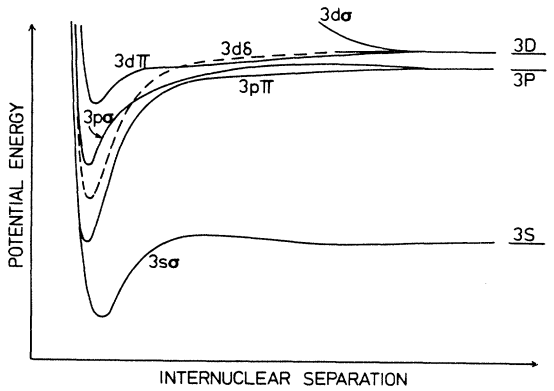

FIG. 6. Interaction potentials (Ref. 9) for several low-lying states of Li-Xe.

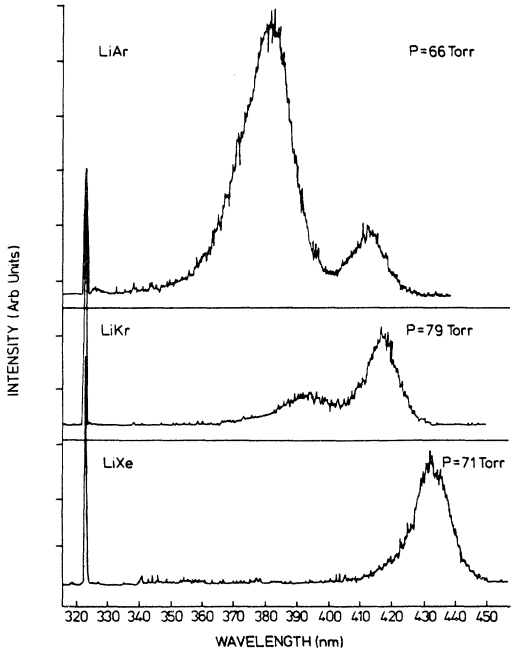

FIG. 7. Collision-induced emission spectra observed in Li-Ar, Li-Kr, and Li-Xe mixtures. The spectra were recorded at rare-gas pressures indicated in the text. The resolution is about 10 Å.

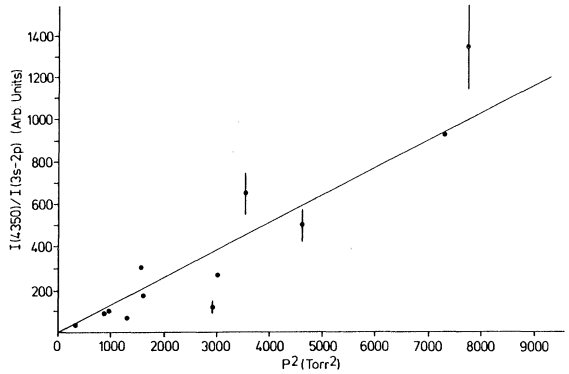

FIG. 8. Peak intensity of the observed $3s\sigma$-$2s\sigma$ Li-Xe collision-induced band vs P^2, where P is the Xe gas pressure. The intensity is measured relative to the atomic Li $3s$-$2p$ transition at 812.7 nm.

served band is largely independent of pressure. As the population of the molecular states is hardly in equilibrium with its atomic source (viz., the P^2 dependence), this may seem surprising. However, for collision-induced emission bands, the emitted intensity can be from a fairly narrow region near the bottom of the well; the shape and peak position would then not depend strongly on R pressure.

In summary, we have presented data on the spectra and pressure dependence of collision-induced continuum emission bands in Li-Ar, Li-Kr, and Li-Xe mixtures. We have also measured rate coefficients for collisional quenching of the atomic Li $3p$ and $3d$ states by all the rare gases.

ACKNOWLEDGMENT

This work was supported by the National Science Foundation and the Research Corporation.

[1]A. C. Tam, G. Moe, W. Park, and W. Happer, Phys. Rev. Lett. 35, 85 (1975).
[2]A. C. Tam, G. Moe, B. R. Bulos, and W. Happer, Opt. Commun. 16, 376 (1976).
[3]R. Novak, N. D. Bhaskar, and W. Happer, J. Chem. Phys. 71, 4052 (1979).
[4]M. A. Islam, A. Kponov, B. Soleman, and W. Happer, Phys. Rev. Lett. 47, 643 (1981).
[5]G. Moe, A. C. Tam, and W. Happer, Phys. Rev. A 14, 349 (1976).
[6]J. P. Visticot, J. Szudy, and B. Sayer, J. Phys. B 14, 2329 (1981).
[7]B. Sayer, M. Ferray, and J. Lozingot, J. Phys. B 12, 227 (1979).
[8]J. Pascale, J. Chem. Phys. 67, 204 (1977).
[9]J. Pascale and J. Vandeplanque, J. Chem. Phys. 60, 2278 (1974).
[10]E. Czuchaj, Z. Phys. A298, 237 (1980).
[11]E. Czuchaj, Z. Phys. A292, 109 (1979).
[12]A. Gallagher, *Metal Vapor Excimers,* Vol. 30 of *Topics in Applied Physics* (Springer, Berlin, 1979).
[13]F. Rostas, in *Alkali—Rare Gas Excimers,* edited by B. Wende (W. de Gruyter, Berlin, 1981).
[14]R. Scheps and A. Gallagher, J. Chem. Phys. 65, 859 (1976).
[15]L. C. Balling, J. J. Wright, and M. D. Havey, Phys. Rev. A 26, 1426 (1982).
[16]W. L. Weise, M. W. Smith, and B. M. Glennon, *Atomic Transition Probabilities,* Natl. Stand. Ref. Data Ser., Natl. Bur. Stand. (U.S.) Circ. No. 4 (U. S. GPO, Washington, D.C., 1971), Vol. 1.
[17]C. Chaleard, B. Dubreuil, and A. Catherinot, Phys. Rev. A 26, 1431 (1982).
[18]G. Ennen and Ch. Ottinger, Chem. Phys. Lett. 88, 487 (1982).
[19]I. Siara, E. S. Hrycyshyn, and L. Krause, Can. J. Phys. 50, 1826 (1972).